Proceedings of ISEC2006
ASME International Solar Energy Conference
July 8-13, 2006, Denver, CO

ISEC2006-99063

A TWO-STEP WATER SPLITTING WITH FERRITE PARTICLES AND ITS NEW REACTOR CONCEPT USING AN INTERNALLY CIRCULATING FLUDIZED-BED

Nobuyuki Gokon
Graduate School of Science and Technology,
Niigata University, 8050 Ikarashi 2-nocho,
Niigata 950-2181, JAPAN

Takayuki Mizuno
Graduate School of Science and Technology,
Niigata University

Shingo Takahashi
Department of Chemistry & Chemical Engineering,
Niigata University,
8050 Ikarashi 2-nocho,
Nigiata 950-2181 JAPAN

Tatsuya Kodama
Department of Chemistry & Chemical Engineering,
Faculty of Engineering,
Niigata University

ABSTRACT

A thermochemical two-step water splitting cycle using a redox system of iron-based oxides or ferrites is one of the promising processes for converting and storing solar energy into a fuel in sunbelt regions. The ZrO_2-supported ferrite (or the ferrite/ZrO_2) powders exhibit superior performances on activity and repeatability of the cyclic reactions when compared to conventional unsupported ferrites. In the first step at 1400˚C under an inert atmosphere, ferrite on ZrO_2 support is thermally decomposed to the reduced phase of wustite that is oxidized back to ferrite on ZrO_2 with steam in a separate second step at 1000˚C. In this paper, a number of ZrO_2-supporetd ferrites, Mn-, Mg-, Co-, Ni- and Co-Mn-ferrites, are examined on activity. The $NiFe_2O_4/ZrO_2$ powder was found to have a greatest activity between them. This paper also describes a new concept of a windowed solar chemical reactor using an internally circulating fluidized bed of ferrite/ZrO_2 particles. In this concept, concentrated solar radiation passes downwards through the transparent window and directly heats the internally circulating fluidized bed. The exploratory experimental studies on this reactor concept are carried out in a laboratory scale for the thermal decomposition of $NiFe_2O_4/ZrO_2$ particle bed as part of two-step water splitting cycle.

INTRODUCTION

Modern solar concentrating systems of the central-tower and dish type systems can provide high-temperature solar thermal energy on levels up to hundreds of megawatts and a few hundred-kilowatts, respectively [1-3], if the system is built in “sunbelt” regions that are greatly insolated, such as the southwest U.S, southern Europe, Australia, and broad regions of the developing world. The reflection and concentration of direct insolation is achieved by sun-tracking mirrors called collectors or heliostats. The concentrated solar radiation is focused on a solar receiver. The maximum concentration factors of these concentrating systems are 1500 to 5000, respectively, while maximum direct insolation frequently reaches $1kWm^{-2}$ in sunbelt regions. The maximum temperatures of the receivers attain up to more than 1500˚C.

The conversion of solar high-temperature heat to chemical fuels has the advantage of producing long-term storable and transportable energy carriers from solar energy. Hydrogen production from water is an important long-term goal in solar fuel production. Various processes for the production of hydrogen by multi-step thermochemical water splitting, such as UT-3, IS and Mark processes, have been proposed and demonstrated [4-7]. However, most of the processes with more than three steps are too complicated for practical solar applications and, they use very corrosive reactant and/or product gases in the presence of steam at high temperatures. This results in difficulties with reactor construction materials.

One of the promising solar thermochemical cycles is a two-step water splitting cycle using a metal-oxide redox pair. This process, originally proposed by Nakamura [8], is as follows:

$$Fe_3O_4 = 3FeO + 1/2O_2 \quad (1)$$

$$3FeO + H_2O = Fe_3O_4 + H_2 \quad (2)$$

This first high-temperature process is highly endothermic while the second process is slightly exothermic at moderate temperatures. The thermodynamic analysis indicates that the solar high-temperature step in the thermal reduction of Fe_3O_4 to FeO (Eq. (1)) proceeds at temperatures above 2500 K under 1 bar [9]. Since the very-high reduction temperature creates engineering challenges, any possibility of lowering the reduction temperature is desirable. The formation temperature of FeO varies with the partial pressure of oxygen in the atmosphere. The iron-oxygen phase diagram by Darken and Gurry [10] shows that the single FeO phase or the FeO + Fe_3O_4 mixed phase can be formed at temperatures from 1300-1400 ºC if the oxygen partial pressure in atmosphere ranges from 10^{-6} to 10^{-8} bar, and that at temperatures above 1400 ºC under these low oxygen partial pressures the liquid iron oxide phase is formed with/without solid Fe_3O_4, since the melting point of FeO is around 1400 ºC. This indicates that the Fe_3O_4-to-FeO thermal reduction of Eq. (1) can proceed to some extent at around 1400ºC if it is performed under an oxygen partial pressure lower than 10^{-6} bar.

As one of the methods of lowering the Fe_3O_4-to-FeO thermal reduction temperature, solid solutions between the redox system Fe_3O_4/FeO and M_3O_4/MO (M = Mn and Co) have been examined using an approach with the possibility of combining good H_2 yields in the Fe_3O_4/FeO system with the low reduction temperature in a M_3O_4/MO [11-14]. Partial substitution of iron in Fe_3O_4 with Mn, Co or Mg is possible to form mixed metal oxides $(Fe_{1-x}M_x)_3O_4$ or ferrites. The mixed oxide may be reducible at lower temperature than that required for the reduction of Fe_3O_4, while the reduced phase $(Fe_{1-x}M_x)_{1-y}O$ is still capable of hydrolysis reaction.

Another problem of the Fe_3O_4/FeO redox pair is rapid deactivation of the iron oxide particles in the cyclic reaction. This is due to the high-temperature melting and sintering in the iron oxide particles. There had been many reports on the two-step water splitting with ferrite particles, such as Mn-ferrite [13] and Ni-Mn-ferrite [14], but no reports had been demonstrated a high activity with good repeatability of the cyclic two-step water splitting by using conventional or “unsupported” ferrite particles. However, the present authors first demonstrated repeatable two-step water splitting by highly-active “ZrO_2-supported” ferrite particles in 2003 [15,16]. The supporting ZrO_2 alleviated coagulating or sintering of the solid reactant of the ferrite, and as a result, the cyclic reaction could be repeated with a relatively good activity in a temperature range of 1000-1400ºC. In comparison the unsupported ferrites did not show such good activity and repeatability on the cyclic reaction.

One of the objectives of this paper is to find the highly reactive ferrites in the ZrO_2-supported powder system. The powder samples of Mn-, Mg-, Ni-, Co-, and Co-Mn-ferrites, supported on ZrO_2, are synthesized and tested on activity.

Another objective of this paper is to propose a new reactor concept using the reactive ZrO_2-suppported ferrite particles as the working materials or solid reactants. The new concept involves using an internally circulating fluidized bed of the ferrite/ZrO_2 particles under direct solar irradiation in a windowed chemical reactor. The exploratory experiments are carried out for the new reactor concept.

NEW REACTOR CONCEPT USING AN INTERNALLY CIRCULATING FLUDIZED-BED

On a parallel with the basic research with respect to active redox working material such as ZrO_2-supported ferrites, a new chemical reactor system needs to be developed to realize the two-step water splitting using concentrated solar radiation as the energy source. The first endothermic step of thermal reduction of redox materials requires very high temperature of about 1300-1400ºC. It is difficult to retain such high temperatures of redox material particles in conventionally heated reactor system using concentrated solar radiation as the energy source. To reach and retain such reaction at high temperatures on the redox working materials in a solar chemical reactor, the redox materials have to be irradiated directly by high fluxes of concentrated solar radiation. From this point of view, some of solar reactor concepts have been proposed or demonstrated for a two-step water splitting by redox materials in the literature.

Recently, it has proposed to use multi-channelled honeycomb ceramic supports coated with active redox material of ferrite powder in a solar receiver-reactor system, in a configuration similar to that encountered in automobile exhaust catalytic converters [17,18]. The ferrite-coated honeycombs are directly irradiated by concentrated solar radiation through a quartz window and heated up to 1200ºC to thermally reduce the redox ferrite coated, while passing an N_2 gas through it. It was reported that solar hydrogen production was feasible by this reactor demonstrating that multi cycling of the process was possible in principle. However, this reactor concept has a disadvantage that mass of the redox materials to be loaded on the honeycomb support is very limited and therefore very small amount of the redox materials, coated on the restricted surface area of the honeycomb support, can contribute the chemical reactions. This factor makes a severe limitation on hydrogen productivity for the reactor. As the result, in order to allow the reactor concept to be upscaled to multi-megawatts scale, a cluster of the reactors has to be constructed on the top of a solar tower [18], but such a system must be very costly and difficult to operate. In addition, a number of the ferrite-coated ceramic honeycombs are very costly.

One of other reactor concepts uses reacting particles fed into a rotating cavity reactor with a window, but it is very complicated and costly to operate [19].

The concept of volumetric gas-particle solar receiver-reactor has been examined for more than a decade [20]. The reactor concept is based on direct solar irradiation of a "suspension" of reacting particles in a gas stream, providing efficient heat transfer directly to a large mass of reacting particles. Thus, one can expect this type of reactors to reveal greater hydrogen productivity than other types mentioned above. However, the difficulty in this type is to allow solar-heated particle suspension to avoid contact with the transparent quartz window. Provided that the reactor is combined with a conventional solar concentrating system such as a solar tower, solar high flux must enter horizontally or upwards into the reactor housing through the window at the side (Fig. 1a). In this case, conventional fluidized beds of reacting particles can not be applied in the solar reactor but a "cloud" of the reacting particles needs to be created by more vigorous gas streams in the reactor to avoid contact between the particles suspension and the window, as shown by Fig. 1a. Several solar reactors of this type were previously constructed and demonstrated using a gas-particle vortex flow confined to a solar cavity receiver with a window [21]. However, the creation of such "particle cloud" or "gas-particle vortex flow" in the reactor makes this reactor concept highly-energy consuming.

However, recently, solar chemical reactors, such as a solar reformer, have been proposed to be combined with a newly developed solar reflective tower or beam-down optics [22, 23]. The optical path comprises a heliostat field illuminating a hyperboloidal reflector that is placed on a tower and directs the beams downwards. This beam-down optics has the advantage over normal tower top arrangement of reactors. This optics allows a large-scale reactor to be built on the ground, and the solar radiation enters the reactor housing through the window in the ceiling. In such a reactor design, conventional fluidized beds of the reacting particles can be applied because interspacing gap will be made between the fluidized particle bed and the window to avoid their contact, as shown by Fig. 1b.

This paper proposes a new reactor concept using an internally circulating fluidized bed of reacting particles. Figure 2 illustrates an example of the prototype reactor. The cylindrical reactor body is made of stainless steel but a transparent quartz window is installed in the ceiling of the reactor. A draft tube is centrally inserted in the fluidized bed region. Gases are introduced into the draft tube and annulus regions in the beds separately. The concentrated solar radiation passes downwards through the window and directly heats the internally circulating fluidized bed of reacting particles. In this system, the particles are always transported upwards in the draft tube and move downwards in the annulus section. This solid circulation within the reactor provides solar energy transfer from the top of the fluidized bed to the bottom since solar-directly-heated particles on the top region always move to the bottom region. This will create a more uniform temperature distribution through the solar-irradiated fluidized bed when compared with a normal fluidized bed solar-irradiated.

This paper reports the first exploratory experiments, using a laboratory-scale quartz tube reactor, on the new solar water-splitting reactor system.

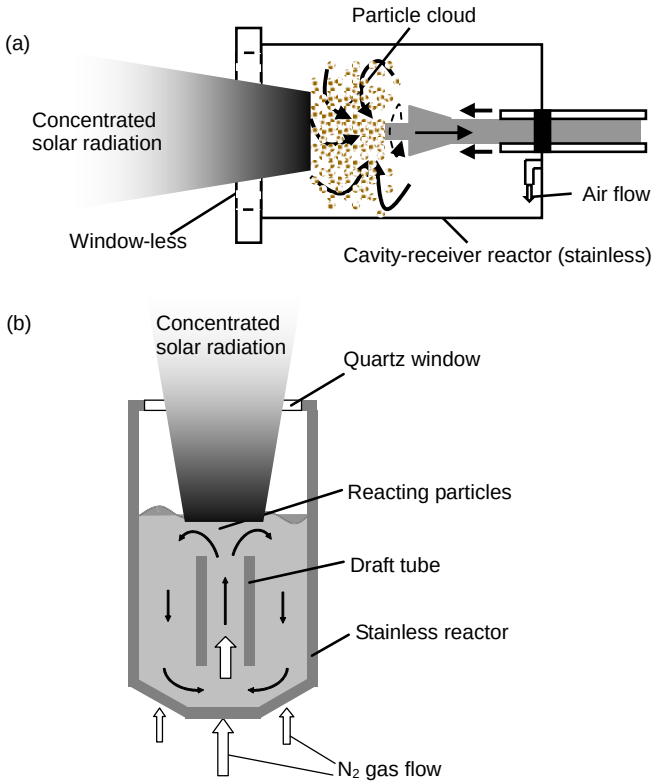

Fig.1 Schematic of solar reactor concepts using (a) "a particle cloud" and (b) "an internally-circulating fluidized bed" of reacting particles.

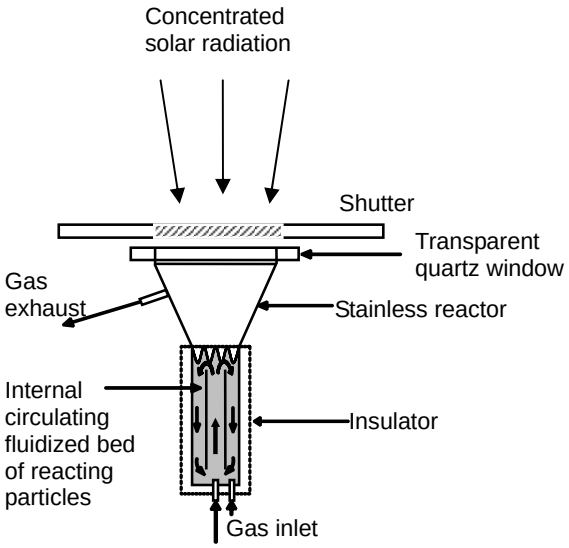

Fig. 2 Schematic of a prototype reactor using an internally circulating fluidized bed of reacting particles

EXPERIMENTAL PROCEDURE

The ZrO_2-supported ferrite powders were subsequent tested with respect to activities for the thermal reduction and the subsequent water decomposition using a quartz reactor chamber and a fix-bed quartz reactor, respectively. In these experiments, the powder samples were heated by an infrared furnace. These series of experiments were focused on determining the most promising ferrite compositions, to be thereafter synthesized in larger quantities and used for testing the internally circulating fluidized bed reactor of quartz tubes under direct irradiation by solar-simulated light from a sun-simulator.

Synthesis of ZrO_2-supported ferrites. The ZrO_2-supported ferrites (Mn-, Mg-, Co-, Ni- and Co-Mn-ferries) were prepared by coating of the ZrO_2-support particles with the ferrite using aerial oxidation method of aqueous suspensions of the Fe(II) hydroxide [15,16]. Ferrite can be plated on a substrate surface of various substances such as organic compounds (PET, PMMA and Teflon), a glass slide and a metal (stainless steel) directly in an aqueous solution of sulfate of an Fe^{2+} ion and those of other bivalent M^{2+} ions (M = Mn, Mg, Ni, or Co) (the aerial Fe^{2+}-oxidation wet method) [24,25]. Hydrolyzed metal ions $FeOH^+$ and MOH^+ in an aqueous solution are adsorbed on a substrate surface which react into ferrite deposits associated with air oxidation of the $FeOH^+$ ion. Thus, here it was expected that ferrite was deposited on the surface of the suspended ZrO_2-support particles by this aerial Fe^{2+}-oxidation wet method. In this work, monoclinic ZrO_2 particles with a 98 % purity were used as the support. The particle size of the ZrO_2 was around 1 μm, and the BET surface area was 12.6 m^2-g^{-1}. The ZrO_2 powder was previously suspended in oxygen- and CO_2-free distilled water. After passing an N_2 for a few hours, appropriate portions of MSO_4 and $FeSO_4$ were dissolved in the solution having ZrO_2 suspension. The solution was adjusted to pH of 8-9 (depending on kinds of metal sulfate) by adding 0.15 mol dm^{-3} NaOH solution to form $M(OH)_2$ and $Fe(OH)_2$. The content of ferrite in the ferrite/ZrO_2 was set to about 20 % on a weight basis. After heating to 65 ºC, air was bubbled through the suspension while keeping the pH of 8-9 by adding 0.15 mol dm^{-3} NaOH solution. The product was collected by centrifuging at 14,000 rpm. After washing with distilled water and then with acetone, it was dried in vacuo at 333 K for a day. The powder was then calcined at 900 ºC in an N_2 atmosphere before use of the high-temperature reactions. Similarly, the non-doped ferrite (Fe_3O_4) was synthesized by the same method mentioned above, except for the use of MSO_4.

To determine the chemical composition of the ferrite phase, the Fe and M contents in the ZrO_2-supported ferrite were determined by dissolving the ferrite phase in an HCl solution and analyzing the solution for Fe and M by atomic emission spectrometry (ICP, Seiko Instrument SPS-1500V).

The samples were subjected to X-ray diffractometry (XRD) with CuK_α radiation (Rigaku, RAD-γA diffractometer) for identification. It was corroborated that only small XRD peaks due to spinel ferrite appeared along with strong peaks of monoclinic ZrO_2 support in the XRD patterns of the ferrite/ZrO_2 samples listed in Table 1. The typical XRD pattern ($Mg_{0.6}Fe_{2.4}O_4/ZrO_2$) was given in Fig. 3.

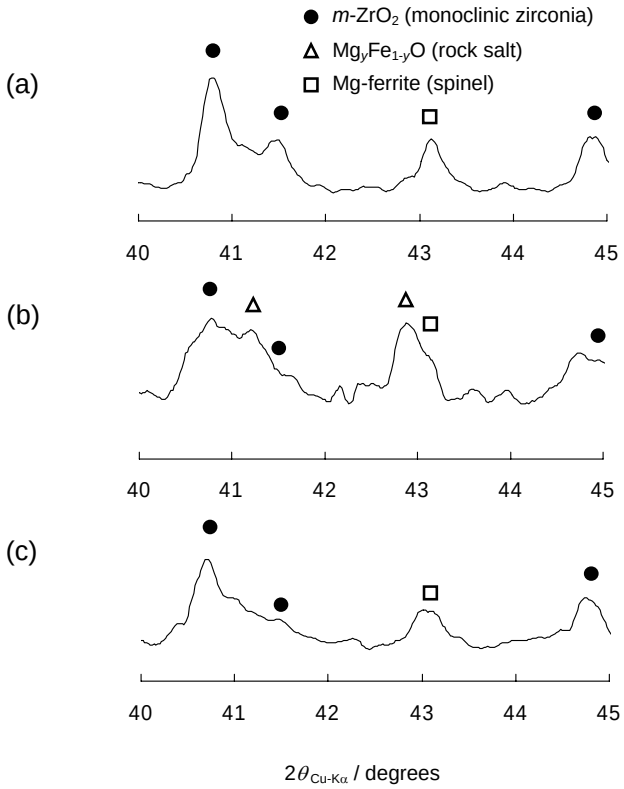

Fig. 3 XRD patterns of (a) $Mg_{0.6}Fe_{2.4}O_4/ZrO_2$ original, (b) that after T-R step, and (c) that after W-O step.

Comparison of activity between ZrO_2-supported ferrites. The ferrite/ZrO_2 powders thus prepared were compared on activity for the two-step water splitting reaction by using a quartz reactor chamber (Fig. 4a) and a fix bed reactor (Fig. 4b). Hereafter the reaction of eq. 1 is referred as the thermal-reduction (T-R) step and the reaction of eq. 2 as the water-oxidation (W-O) step. The experimental set-up of the quartz reactor chamber with fixed bed for the T-R step is illustrated in Fig. 4a. The ZrO_2-supported ferrite sample (0.7-1.0 g) was mounted in a platinum cup (10-mm diameter and 7-mm long), and it was placed on the ceramic bar in the quartz reactor chamber with an inner diameter of 45 mm (ULVAC-RICO, SSA-E45). While passing an N_2 gas stream (99.999 %-N_2) at a flow rate of 1.0 Ndm^3 min^{-1}, the cup was heated up to 1400ºC within 10 min in an infrared furnace (ULVAC-RIKO, RHL-VHT-E44). The temperature was controlled using a R-type thermocouple in contact with the platinum cup. After heating the sample at a constant temperature for 30 min, it was cooled to room temperature. After the T-R step, the thermally-reduced solid sample was pulverized by using a pestle and a mortar. The

pulverized solid sample was packed in the fixed-bed reactor of a quartz tube with an inner diameter of 7 mm (Fig. 4b) in order to perform the water-oxidation (W-O) step. An H_2O/N_2 gas mixture was introduced into the reactor. The H_2O/N_2 gas mixture was produced by passing N_2 gas through the distilled water at 80 ºC at an N_2 flow rate of 4 Ncm^3 min^{-1}. The partial pressure of steam in the H_2O/N_2 mixture was estimated to be 0.47 atm from the steam vapor pressure at 80 ºC and at 1 atm. The reactor was heated up to 1000 ºC in an infrared furnace (ULVAC-RIKO, RHL-E45P) within 10 min. The temperature was controlled using a K-type thermocouple in contact with the sample bed located inside the reactor. The W-O step was performed at 1000 ºC for 50 min. To determine the amounts of hydrogen evolved during the W-O step, the effluent was collected in a bottle by water displacement. After the W-O step, the volume of the collected effluent was measured and the gas compositions were determined by gas chromatography with a TCD detector (Shimadzu, GC-4C). The T-R and W-O steps were alternately repeated 4-6 times. The thermally-reduced solid sample was pulverized again after every cycle.

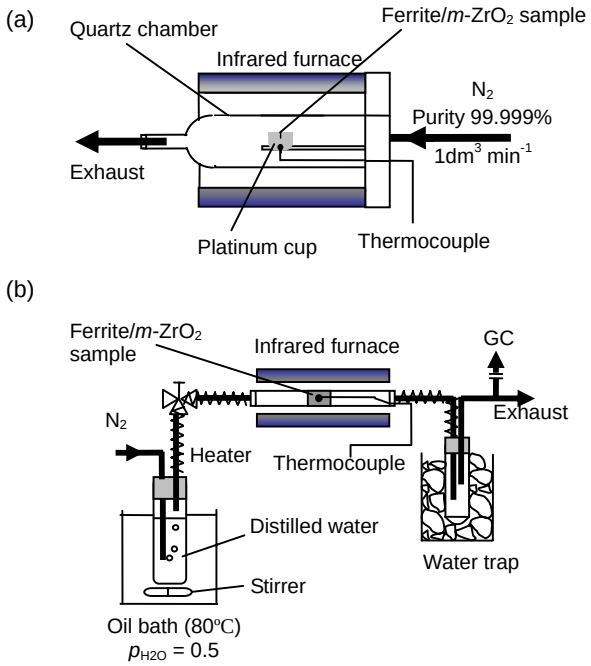

Fig. 4 Experimental setups for a) the thermal-reduction (T-R) step and b) the water-oxidation (W-O) step.

More than two replicates were used for each ferrite/ZrO_2 sample to check for reproducibility. The averages of hydrogen amounts produced in repeated cycles were compared between the replicates and for each sample the relative standard deviation in the replicates were below 10%.

The solid samples were subjected to X-ray diffractometry (XRD) with CuK_α radiation (MAC Science, MX-Labo) for identification.

Set-up and exploratory testing of the internal circulating fluidized bed reactor. The internal circulating fluidized bed reactor used is illustrated in Fig. 5a. The reactor was made of quartz tubes. The diameter of the outer tube was 45 mm (inside diameter 40 mm) with 2.5 mm thickness. The diameter of the inner draft tube, that was centrally located, was 20 mm with 2.5 mm thickness and the tube length was 10 mm. The bottom of the draft tube was positioned at 11 mm above from a porous quartz frit of distributor. In addition, a conical-shaped quartz cap tube (the inside diameter of the top was 6 mm and that of the bottom was 11 mm) (Fig. 5b) was fixed on the distributor to make a faster flow of carrier gas in the draft tube than that in the outer annular section. The carrier gas was allowed to flow upwards through the tubes to make an internal circulating fluidized bed of the ZrO_2-supported ferrite particles. 20-40 grams of the ZrO_2-supported $NiFe_2O_4$ particles was loaded in the reactor. The static bed height varied from 20 to 40 mm depending on the mass of the particles.

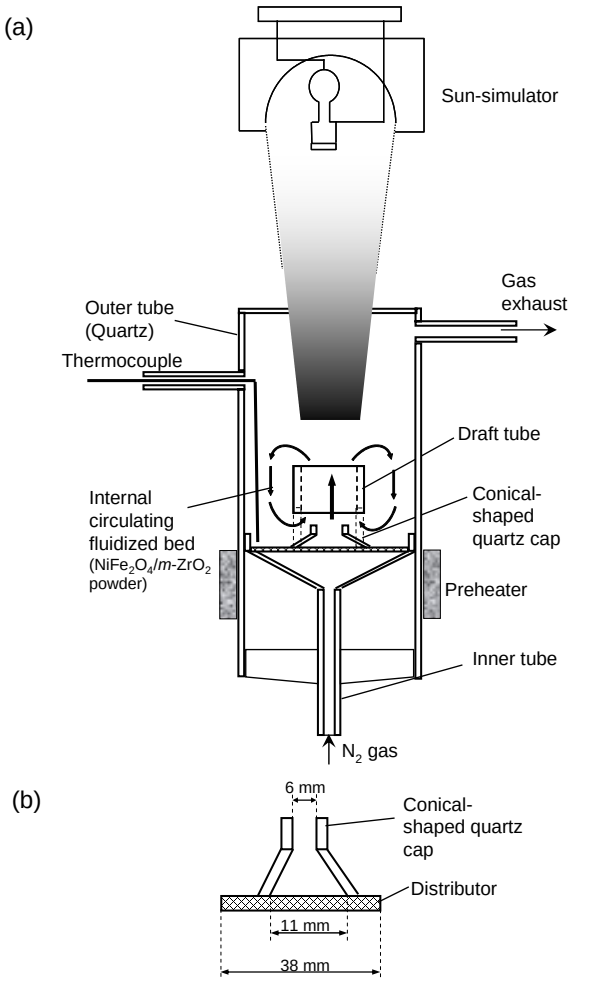

Fig. 5 Schematic of (a) the experimental set-up for an internally circulating fluidized bed reactor with draft tube and (b) the conical-shaped cap.

This internal circulating fluidized bed reactor was placed below a 6-kW Xe-arc lamp of the sun-simulator (NIHON KOKI, UXL-6000H) with the central axis of the reactor along with the axis of the oval concentrator of the sun-simulator (Figure 6: photo). The top of the static bed was set on the focal spot and the focal diameter of the spot varied from 4-5 cm. The concentrator of the sun-simulator reflected the Xe-lamp beam downwards to the focal spot. The intensity and distribution of the concentrated Xe-lamp beam on the spot could be varied by changing the power supply to the Xe-arc lamp or by changing the focus diameter of the spot. The energy flux densities of the Xe-lamp beam on the spot were previously measured by using heat flux transducer with a sapphire window attachment (Medtherm, 64-100-20/SW-1C150).

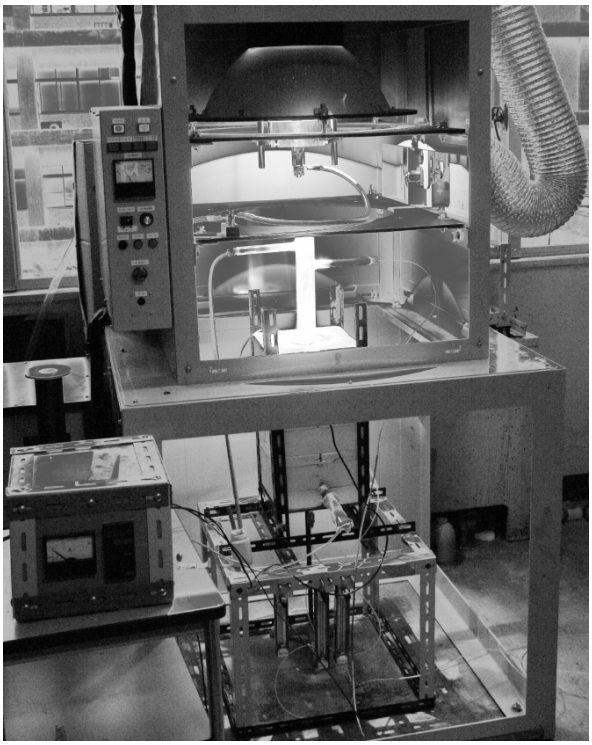

Fig. 6 The internal circulating fluidized bed reactor in the sun-simulator.

An N_2 gas stream (99.999 %-N_2) was introduced as a carrier gas from the bottom of the reactor to make an internal circulating fluidized bed of the $NiFe_2O_4/ZrO_2$ particles. The reactor was preheated by a cylindrical electric furnace up to 900ºC. The preheater was controlled using a R-type thermocouple in contact with the exterior reactor wall. While passing an N_2 gas stream at a flow rate of 1.0-5.0 $Ndm^3\ min^{-1}$, the internally circulating fluidized bed was directly irradiated and heated with the concentrated Xe-lamp beam from the sun-simulator. The bed temperature at the bottom of the annular section was measured by using a K-type thermocouple inserted into the reactor.

After irradiation, the fluidized bed was cooled to room temperature. The solid samples were analyzed by using X-ray diffractometry (XRD) with CuK_α radiation (MAC Science, MX-Labo) for identification. A portion of the thermally-reduced $NiFe_2O_4/ZrO_2$ particles was taken out (1 g) from the reactor and subject to the W-O step for determining the hydrogen productivity under the same reaction condition of the above-mentioned activity test.

RESULTS AND DISCUSSION

Activity of ZrO_2-supported ferrites. The ferrite/ZrO_2 samples tested in this work are listed in Table 1. About 1 gram of the sample in the platinum cup in the reaction chamber of Fig. 5a was heated up to 1400˚C to thermally reduce the ferrite phase on ZrO_2 support (T-R step). Compared to the unsupported ferrite sample that sintered significantly and became a dense and hard mass in the platinum cup after T-R step [16], after the thermal reduction, the ferrite/ZrO_2 samples became a porous pellets or porous aggregates. The pellet or aggregate could be easily pulverized using a pestle and a mortar. The result indicates that the ZrO_2-supporting is effectively alleviated the high-temperature sintering of iron oxides in the various ferrite systems. The pulverized solid sample underwent the W-O step at 1000˚C in the fixed bed reactor of Fig. 5b. Figure 7 shows hydrogen amounts produced in the W-O steps of the repeated water splitting cycle using the ferrite/ZrO_2 sample. The hydrogen amounts produced per weight of used solid material (the ferrite phase + ZrO_2 support) are plotted with respect to run number of the cycle. For each run, the average value of the replicates is plotted here.

Table 1 Composition and loading of the ZrO_2-supported ferrites tested

Notation	Composition	Loading / wt %
non doped	Fe_3O_4/*m*-ZrO_2	20.0
Mn04	$Mn_{0.36}Fe_{2.64}O_4$/*m*-ZrO_2	17.0
Mn07	$Mn_{0.69}Fe_{2.31}O_4$/*m*-ZrO_2	19.0
Mn10	$MnFe_2O_4$/*m*-ZrO_2	19.0
Mg02	$Mg_{0.19}Fe_{2.81}O_4$/*m*-ZrO_2	17.0
Mg06	$Mg_{0.56}Fe_{2.44}O_4$/*m*-ZrO_2	18.8
Co02Mn05	$Co_{0.19}Mn_{0.48}Fe_{2.33}O_4$/*m*-$ZrO_2$	19.4
Co04Mn01	$Co_{0.39}Mn_{0.10}Fe_{2.51}O_4$/*m*-$ZrO_2$	16.8
Co04Mn03	$Co_{0.39}Mn_{0.30}Fe_{2.31}O_4$/*m*-$ZrO_2$	15.7
Co04Mn05	$Co_{0.39}Mn_{0.52}Fe_{2.09}O_4$/*m*-$ZrO_2$	15.5
Co06Mn02	$Co_{0.56}Mn_{0.16}Fe_{2.28}O_4$/*m*-$ZrO_2$	18.0
Co04	$Co_{0.42}Fe_{2.58}O_4$/*m*-ZrO_2	16.7
Co07	$Co_{0.67}Fe_{2.33}O_4$/*m*-ZrO_2	20.2
Co10	$CoFe_2O_4$/*m*-ZrO_2	20.1
Ni10	$NiFe_2O_4$/*m*-ZrO_2	19.2

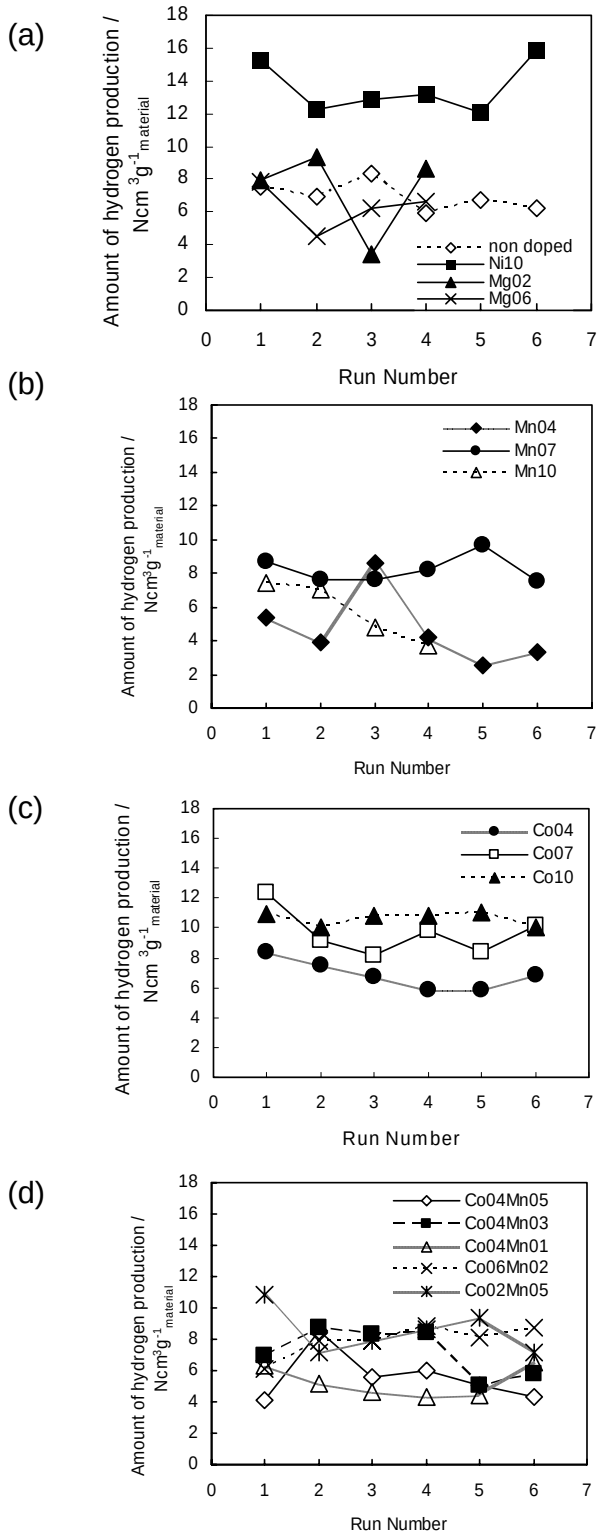

Fig. 7 Hydrogen production per 1 gram of the sample for run of the W-O step: (a) Fe_3O_4, $NiFe_2O_4$ and $Mg_xFe_{3-x}O_4$ (x = 0.2 and 0.6), (b) $Mn_xFe_{3-x}O_4$ (x = 0.4, 0.7, and 1.0), (c) $Co_xFe_{3-x}O_4$ (x = 0.4, 0.7, and 1.0) and (d) $Co_xMn_yFe_{3-x-y}O_4$.

Table 2 Hydrogen production and ferrite conversion of the ZrO_2-supported ferrites

Notation	Runs of cyclic reaction	Average of hydrogen production / $Ncm^3g^{-1}_{material}$	Ferrite conversion[a] / %
non doped	6	6.9	33
Mn04	6	4.7	26
Mn07	6	8.2	41
Mn10	4	5.7	28
Mg02	4	7.3	40
Mg06	4	6.2	29
Co02Mn05	6	8.5	42
Co04Mn01	6	5.2	30
Co04Mn03	6	7.2	44
Co04Mn05	6	5.6	34
Co06Mn02	6	7.9	42
Co04	6	6.8	39
Co07	6	9.7	46
Co10	6	10.6	51
Ni10	6	13.6	69

[a]Estimated from the hydrogen amount evolved in the subsequent W-D step assuming that the wustite phase formed in the T- R step was completely reoxidized to ferrite via the water decomposition.

The cycle was repeated by 4-6 times for each sample and the hydrogen amount produced per one cycle was estimated from the average of the repeated cycles. For each sample, the average of the hydrogen production, per cycle and per sample weight (the ferrite phase + ZrO_2 support) are listed in Table 2.

As can be seen in Fig. 7a and Table 2, the activity of the ferrite/ZrO_2 was scarcely promoted by Mg-doping into the ferrite phase. The hydrogen production did not increase in the $Mg_xFe_{3-x}O_4/ZrO_2$ sample in comparison to non-doped Fe_3O_4/ZrO_2. The activity was, however, greatly promoted by Ni-doping into the ferrite phase. About double the amount of hydrogen could be produced by $NiFe_2O_4/ZrO_2$ in comparison to non-doped Fe_3O_4/ZrO_2.

In the case of $Mn_xFe_{3-x}O_4/ZrO_2$ (Fig. 7b), the increased product hydrogen amount was observed for the sample with x = 0.7. But it was only 1.2 times larger than non-doped Fe_3O_4/ZrO_2. In the case of $Co_xFe_{3-x}O_4/ZrO_2$ (Fig. 7c), the activity was improved over x = 0.7 in the ferrite phase. Especially, for the sample with x = 1.0, the product hydrogen amount increased by about 1.5 times compared with non-doped one.

Co-Mn-ferrites or $Co_xMn_yFe_{3-x-y}O_4$, supported on ZrO_2, were also tested (Fig. 7d) and it was found that $Co_{0.2}Mn_{0.5}Fe_{2.3}O_4$ could increase the product hydrogen amount to some extent, only by about 1.2 times compared with non-doped one.

The conversion from ferrite to wustite phase on ZrO_2 in the T-R step was estimated from the hydrogen amount produced in the subsequent W-O step assuming that the wustite phase

formed in the T-R step was completely reoxidized to ferrite via water decomposition in the subsequent W-O step. The estimated ferrite conversions on the average of the repeated cycles are also listed in Table 2. As can be seen here, the ferrite conversion reached to about 69 % with the $NiFe_2O_4/ZrO_2$.

From these series of experiment, the most promising ferrite composition on ZrO_2 support was found to be $NiFe_2O_4$. Therefore, $NiFe_2O_4/ZrO_2$ particles were synthesized in larger quantities and used for testing the internally circulating fluidized bed reactor of quartz tubes as described below.

Exploratory testing of the internal circulating fluidized bed reactor. About 20 grams of the $NiFe_2O_4/ZrO_2$ sample was loaded in the internally circulating fluidized bed reactor (Fig. 5a), and the T-R step of the sample was carried out by Xe-beam-irradiating the internally circulating fluidized bed of the $NiFe_2O_4/ZrO_2$ particles.

First, to compare the internal circulating fluidized bed design (Fig. 5a) with a reactor without the draft tube (a normal fluidized bed reactor), the thermal reduction of the $NiFe_2O_4/ZrO_2$ sample was performed using the same quartz reactor but without the draft tube. In this case a normal fluidized bed of the $NiFe_2O_4/ZrO_2$ particles was made in the bed region and irradiated by the concentrated Xe-beam in the reactor. After irradiating for 120 min and then cooling to room temperature, a small portion of the thermally-reduced solid sample (about 1 gram) was taken from the bed in the reactor, and loaded in the another fix bed reactor of Fig. 4b to perform the W-O step. The reaction conditions of the experiment and the hydrogen production amount in the W-O step are given in Table 3. The hydrogen amount produced was very small and the ferrite conversion in the T-R step, estimated from the hydrogen production in the subsequent W-O step, was only 1 %. The bed temperature at the bottom of the annular section during the irradiation ranged from 900 to 1000 ˚C.

Table 3 Comparison of hydrogen production between the internally-circulating fluidized bed and the normal fluidized bed reactor.

Sample Weight / g	Total radiating time / min	Input energy / kW	Amount of hydrogen/ $Ncm^3g^{-1}_{-material}$	Ferrite conversion / %
21.5	120	0.82 (1110 kW/m²)[a]	0.23	1.1
24	60	0.82 (1110 kW/m²)[a]	3.4	15.3

[a]Maximum energy flux density of the incident beam at the central position of the spot.

The thermal reduction of the $NiFe_2O_4/ZrO_2$ was then tested using the reactor with the draft tube under the same reaction conditions. The internally circulating fluidized bed of the sample was irradiated only for 60 min by the concentrated Xe-beam, but the ferrite conversion estimated increased to 15% (Table 3). In this case, the bed temperature at the bottom of the annular section during the irradiation ranged from 1000 to 1200 ˚C. This indicates that the internal circulation of the particles with the draft tube effectively enhances the heat transfer from the top to the bottom of the bed. Consequently, the bed temperature after irradiating was increased from 900-1000 ˚C (a normal fluidized bed reactor) to 1000-1200 ˚C (the internal circulating fluidized bed design).

In the next experiment, the intensity of the irradiating Xe-beam flux was increased in order to improve the ferrite conversion of the $NiFe_2O_4/ZrO_2$ sample in the thermal reduction. The input power of the incident Xe-beam into the reactor was allowed to increase from 0.82 to 1.18 kW, and the central or peak flux density of the focal spot increased from 1110 to 2960 kW-m^2. The experimental conditions and the results are given in Table 4. After irradiating the internally circulating fluidized bed of the $NiFe_2O_4/ZrO_2$ particles for 30 min and then cooling to room temperature, 1 gram of the thermally-reduced solid sample was taken from the bed region, and tested on the activity for the W-O step in the fix bed reactor. The hydrogen amount produced significantly increased in comparison to the previous case in Table 3, and the estimated ferrite conversion in the T-R step reached up to 29 %. The Xe-beam irradiation of the fluidized $NiFe_2O_4/ZrO_2$ bed was restarted and it continued for another 30 min (the total irradiation period of time was 60 min). After the irradiation, the W-O step was curried out by 1 gram of the thermally reduced sample in the same matter as above. As given in Table 4, the ferrite conversion of the solid sample increased to 45 %. When the total irradiation time increased to double, the ferrite conversion does not reach double but about 1.6 times. This indicates that the reaction rate of thermal-reduction of the fluidized $NiFe_2O_4/ZrO_2$ sample decayed with increasing the irradiating time.

Table 4 Hydrogen production amount by the internal circulating $NiFe_2O_4/ZrO_2$ fluidized bed reactor.

Total Irradiating time / min	Input energy / kW	Amount of hydrogen / $Ncm^3g^{-1}_{-material}$	Ferrite conversion / %
30	1.18 (2964kW/m²)[a]	6.0	28.5
60	1.18 (2964kW/m²)[a]	9.5	45.2

[a]Maximum energy flux density of the incident beam at the central position of the spot.

Figure 8 shows the change of the XRD pattern of the $NiFe_2O_4/ZrO_2$ sample when the ferrite conversion was 45 %. As can be seen in Figs. 7a and b, after 60 min of irradiation in total, in the XRD pattern of the $NiFe_2O_4/ZrO_2$, the reflection peaks due to $NiFe_2O_4$ became less intense in comparison with those in the original $NiFe_2O_4/ZrO_2$, and a small XRD peak of

the (200) reflection due to wustite appeared along with strong peaks of ZrO_2 support (monoclinic). This wustite peak disappeared after the W-O step (Fig. 7c) and the spinel ferrite peaks became intense again. These results indicate that the hydrogen production observed here was associated with the redox reaction of Ni-ferrite phase on ZrO_2 support.

In this paper, the present authors examined and compared the reactivity of ferrite/*m*-ZrO_2 with many other kinds of metal-doped ferrite/*m*-ZrO_2 systems, such as Mn-ferrites, Mg-ferrites, Co-ferrites, Ni-ferrites and Co-Mn ferrites. As the results, it has found that this $NiFe_2O_4$/*m*-ZrO_2 has the greatest reactivity between them. Further, the present authors have examined and compared the reactivity of ferrite/cubic ZrO_2 stabilized with high yttrium content (YSZ). The new redox reaction has found to occur in the Fe_3O_4/YSZ with more than 8 mol%-Y_2O_3 in YSZ for the two-step water splitting reaction. These detailed data will be published elsewhere.

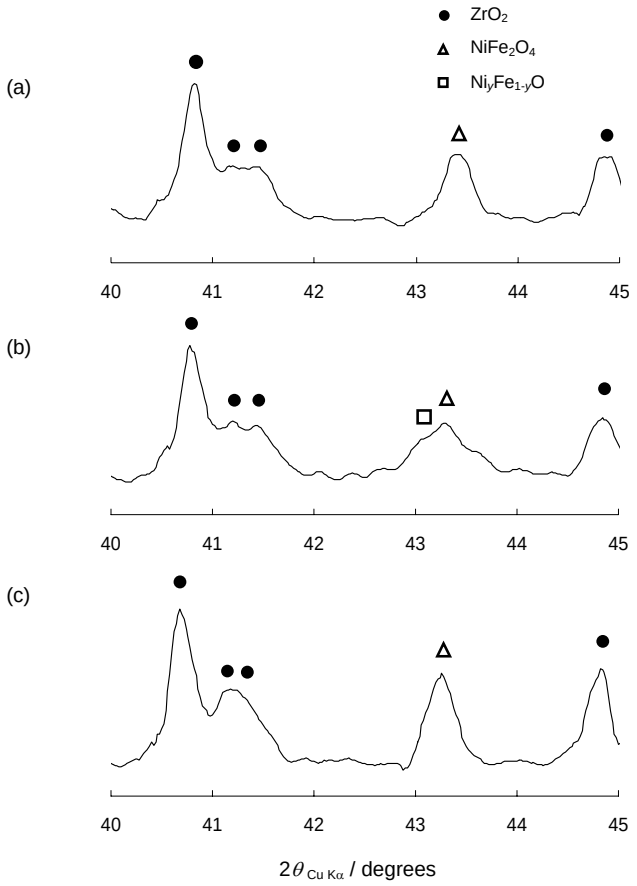

Fig. 8 XRD patterns of the $NiFe_2O_4/ZrO_2$ samples; (a) original, (b) after the T-R step by the internally circulating fluidized bed reactor and (c) after the subsequent W-O step.

SUMMARY

The ZrO_2-supported $NiFe_2O_4$ is found to be the promising material for a two-step water splitting with the superior activity and repeatability below 1400 ˚C. The new concept of a windowed solar chemical reactor using an internally circulating fluidized bed of ferrite/ZrO_2 particles is proposed and demonstrated using $NiFe_2O_4$//ZrO_2 particles and a laboratory-scale quartz tube reactor. Through the direct irradiation of the fluidized $NiFe_2O_4$//ZrO_2 bed by the solar-simulated, high flux beam, about 45 % of the $NiFe_2O_4$ could be converted to the reduced phase that was completely reoxidized with steam at 1000˚C to generate hydrogen.

REFERENCES

[1] Kalogirou, A. S., 2004, “Solar thermal collectors and applications”, Progress in Energy and Combustion Science, **30**, pp. 231-295.

[2] Mills, D., 2004, “Advances in solar thermal electricity technology”, Solar Energy, **76**, pp. 19-31.

[3] Johnston, G., Lovegrove, K., Luzzi, A., 2003, “Optical performance of spherical reflecting elements for use with paraboloidal dish concentrators”, Solar Energy, 74, pp. 133-140.

[4] Bilgen, E., and Joels, R. 1985, “An assessment of solar hydrogen production using the Mark 13 hybrid process,” Int. J. Hydrogen Energy. **10**(3), pp. 143-155.

[5] Onuki, K., Shimizu, S., Nakajima, H., Fujita, S., Ikezoe, Y., Sato, S., and Machi, S., 1990, “Studies on an iodine-sulfur process for thermochemical hydrogen production,” *Proc. the 8th World Hydrogen Energy Conference* (Hawaii, 1990), Vol. 2, pp. 547-556.

[6] Sakurai, M., Bilgen, E., Tsutsumi, A., and Yoshida, K., 1996, “Solar UT-3 thermochemical cycle for hydrogen production,” Solar Energy, **57**(1), pp. 51-58.

[7] Funk, J. E., 2001, “Thermochemical hydrogen production: past and preset,” Int. J. Hydrogen Energy, **26**, pp. 185-190.

[8] Nakamura, T., 1977, “Hydrogen production from water utilizing solar heat at high temperatures,” Solar Energy, **19**, pp. 467-475.

[9] Kodama, T., 2003, “High-temperature solar chemistry for converting solar heat to chemical fuels,” Progress in Energy and Combustion Science, **29**, pp. 567-597.

[10] Darken, L. S., Gurry, R. W., 1946, “The system iron-oxygen. Ⅱ. Equilibrium and Thermodynamics of Liquid Oxide and Other Phase,” J. Am. Chem. Soc., 63, pp. 798-816.

[11] Lundberg, M. 1993, “Model calculations on some feasible two-step water splitting processes,” Int. J. Hydrogen Energy, **18**(5), pp. 369-376.

[12] Ehrensberger, K., Frei, A., Kuhn, P., Oswald, H., and Hug, P., 1995, “Comparative experimental investigations of the water-splitting reaction with iron oxide $Fe_{1-y}O$ and iron manganese oxides $(Fe_{1-x}Mn_x)_{1-y}O$,” Solid State Ionics, **78**, pp. 151-160.

[13] Ehrensberger, K., Kuhn, P., Shklover, V., and Oswald, H., 1996, “Temporary phase segregation processes during the

oxidation of $(Fe_{0.7}Mn_{0.3})0_{.99}O$ in N_2-H_2O atmosphere," Solid State Ionics, **90**, pp. 75-81.
[14] Tamaura, T., Steinfeld, A., Kuhn, P., and Ehrensberger, K., 1995, "Production of solar hydrogen by a novel, 2-step, water-splitting thermochemical cycle," Energy, **20**(4), pp. 325-330.
[15] Kodama, T., Kondoh, Y., Kiyama, A., and Shimizu, K-I., 2003, "Hydrogen production by solar thermochemical water-splitting/methane-reforming process," *Proceeding of ASME International Solar Energy Conference (ISEC) 2003* (Hawaii, 2003), M. D. Thornbloom, and S. A. Jones, eds., ASME, New York, ISEC2003-44037 (CD-ROM publication).
[16] Kodama, T., Kondoh, Y., Yamamoto, R., Andou, H., and Satoh, N., 2005, "Thermochemical Hydrogen production by a redox system of ZrO_2-supported Co(II)-ferrite," Solar Energy, 78, 623-631.
[17] Agrafiotis, C., Roeb, M., Konstandopoulos, A.G., Nalbandian, L., Zaspalis, V.T., Sattler, C., Stobbe, P., Steele, A.M., 2005, "Solar water splitting for hydrogen production with monolithic reactors," Solar Energy, 79, 409-421.
[18] Roeb, M., Sattler, C., Klüser, R., Monnerie, N., Oliveira, L., Konstandopoulos, A.G., Agrafiotis, C., Zaspalis V.T., Nalbandian, L., Steele, A., Stobbe, P., 2005, "Solar hydrogen production by a two-step cycle based on mixed iron oxides," *Proceeding of ASME International Solar Energy Conference (ISEC) 2005* (Orlando, Florida, 2005), ASME, New York, ISBN: 0-7918-3765-3, ISEC2005-76126 (CD-ROM publication).
[19] Haueter, P., Moeller, S., Palumbo, R., Steinfeld, A., 1999, "The production of zinc by thermal dissociation of zinc oxide – solar chemical reactor design," Solar Energy, 67(1-3), 161-167.
[20] Meier, A., Ganz, J., Steinfeld, A., 1996, "Modeling of a novel high-temperature solar chemical reactor," Chemical Engineering Science, 51(11), 3181-3186.
[21] Weidenkaff, A., Brack, M., Möller, S., Palumbo, R., Steinfeld, A., 1999, "Solar thermal production zinc: Program strategy and status of research," J. Phys. IV France, 9, Pr3-313-Pr3-318.
[22] Segal, A., and Epstein, M., 2000, "The optics of the solar tower reflector," Solar Energy, **69** (Suppl.), pp. 229-241.
[23] Segal, A., and Epstein, M., 2003, "Solar ground reformer," Solar Energy, **75**, pp. 479-490.
[24] Abe, M., Tanno, Y., and Tamaura, Y., 1985, "Direct formation of ferrite film in wet process," J. Appl. Phys., **57**(1), pp. 3795-3797.
[25] Tamaura, Y., Abe, M., Itoh, T., 1987, "Magnetic thin film formation reaction of ferrite in aqueous solution," J. Chem. Soc. Jpn, No. 11, pp. 1980-1987